Comparative Analysis of Vernier Machines with Spoke, Surface Mounted, and Halbach PM Rotors for In-wheel Traction

Ali Mohammadi[1], Aaron M. Cramer[2], and Dan M. Ionel[1]
[1]SPARK Laboratory, Stanley and Karen Pigman College of Engineering, University of Kentucky, Lexington, KY, USA
[2]ECE Department, Stanley and Karen Pigman College of Engineering, University of Kentucky, Lexington, KY, USA
alimohammadi@uky.edu, aaron.cramer@uky.edu, and dan.ionel@ieee.org

***Abstract*—Axial-flux Permanent Magnet (AFPM) machines are well-suited for in-wheel traction in electric vehicles due to their compact structure and higher torque density. This paper presents a large-scale design optimization of an axial-flux permanent magnet vernier machine (PMVM) of the MAGNUS type with a double stator configuration. The active stator features double-layer wound coils, while the passive stator is unwound but has a similar profile. The reference design employs a rotor with permanent magnets (PMs) arranged in a spoke-type field-intensifying pattern, providing high flux concentration. Design optimization was performed using 3-D electromagnetic Finite Element Analysis (FEA) and the Differential Evolution (DE) algorithm. A best design from the Pareto front was selected, and a comparative study was conducted by replacing the spoke-type rotor with a Halbach array and a surface-mounted PM (SPM) rotor. The performance of the machine, considering these proposed rotor types was assessed for traction requirements. The results indicate that the spoke configuration is superior in terms of power density, efficiency, cost of active material, and having a higher constant power region.**

***Index Terms*—Axial-flux vernier machine, spoke, Halbach, surface mounted, finite element analysis, flux weakening, electrical vehicles, in-wheel motor, design optimization.**

I. Introduction

The transition towards electric vehicles (EVs) in the transportation sector marks a significant transformation, causing profound changes in the energy industry. This shift may influence climate change and the sustainable utilization of existing resources [1]. The traction system of EVs plays a pivotal role in this transition, necessitating innovative solutions that strike a balance between compact design, high efficiency, and reliable performance [2], [3].

Permanent magnet synchronous machines (PMSM) with high specific torque and efficiency especially those of the axial flux type, are currently being studied and developed for diverse systems such as HVAC, aviation propulsion, and electric vehicle. Axial-flux permanent magnet motors have emerged as promising candidates for in-wheel traction due to their inherent advantages of a compact structure and high torque density. Direct-drive systems employing in-wheel motors eliminate mechanical transmission components, resulting in lower vibration and noise levels, higher efficiency, and more flexible vehicle wheel control [4]–[7].

In-wheel motors for EVs benefit from efficient energy conversion, minimized mechanical losses, and flexibility of multiple driving modes. In contrast to conventional vehicles featuring a single centrally located motor, EVs equipped with four independently driven in-wheel motors demonstrate superior transmission efficiency [8].

Among different AFPM topologies, vernier machines have been reported for direct drive and high torque density applications. Various designs have been investigated to address different operational aspects. A general review on direct drive electric machines for EV application identified a trade-off between power factor and torque density in vernier machines [9]. This trade-off has also been studied in vernier machines with surface-mounted PM rotors for direct-drive applications [10], where a segmented-stator has been introduced to improve average torque and power factor.

High torque density vernier machines with an outer rotor and inner stator structure using Halbach array PMs have been reported in [11]. A comparative study of vernier machines shows that a design with spoke-type PM rotor has more torque capability and less PM loss compared to the surface-mounted PM rotor [12]. Earlier developments of spoke rotors with magnetic flux concentration have been described for example in [13], [14]. The effectiveness of spoke, surface-mounted, and Halbach PM rotors has been studied in machines with high flux concentration and torque density, covering various applications and topologies, including direct-drive wind turbine generators, magnetic gears, and electric vehicles [15]–[19].

The high PM to armature winding pole ratio in vernier machines result in higher flux concentration and higher electromagnetic torque [20]. A comparison for radial flux vernier machines with multiple rotor topologies with the same stator is reported in [8]. The advantages of vernier machines with spoke-type rotors are high magnetic polarities providing opportunities for high flux concentration, combined with a very low number of stator coils, which may simplify the manufacturing of stator windings [5], [21]–[23].

In studies focusing on the radial-flux, dual-stator, spoke-type PMVM, as detailed in [24], [25], emphasis was placed on its high torque density and power factor. To increase the torque density in permanent magnet vernier machines, different topologies including Halbach PMs, dual-rotor, dual-stator, and PMs positioned on both sides of the rotor and stator have been proposed in recent years [26], [27].

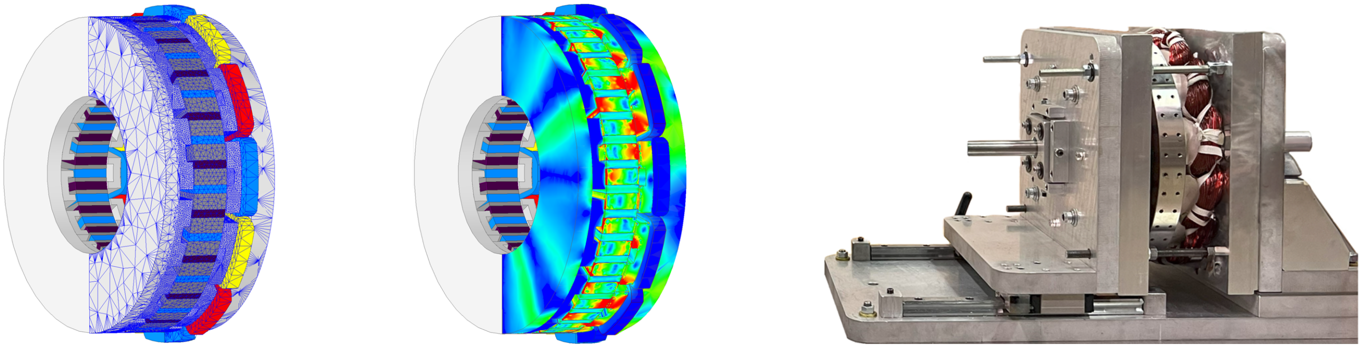

(a) (b) (c)

Fig. 1. The reference axial-flux PM vernier machine with spoke-type rotor for in-wheel traction. (a) Mesh elements of the 3-D FE model. (b) Magnetic flux density map at the rated loading. (c) The assembled prototype of the machine which serves as a calibrated model.

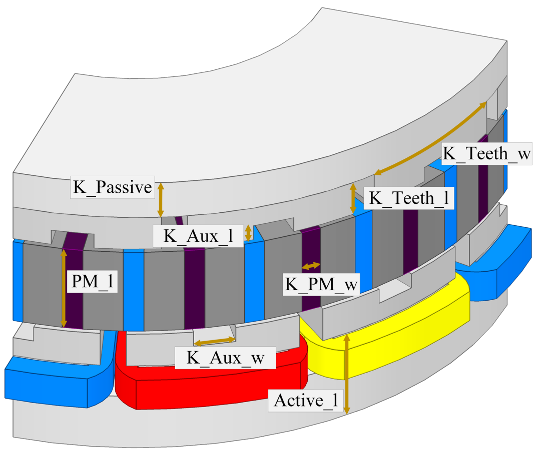

Fig. 2. Independent variables employed in the optimization on the minimum periodicity region of the spoke-type design.

TABLE I
INDEPENDENT VARIABLES USED FOR THE OPTIMIZATION, THEIR DESCRIPTION BASED ON DESIGN SPECIFICATIONS, AND CORRESPONDING RANGES USED BY THE OPTIMIZATION ALGORITHM.

NO	Variable	Ratio/Length	Min	Max
1	*k_Teeth_l*	teeth length	0.45	0.80
2	*k_Teeth_w*	teeth width	0.20	0.40
3	*PM_l*	PM length [mm]	19.0	50.0
4	*k_PM_w*	PM width	0.35	0.90
5	*k_Aux_l*	Auxiliary teeth length	0.25	0.70
6	*k_Aux_w*	Auxiliary teeth width	0.50	0.85
7	*Active_l*	Active stator [mm]	29.5	56.0
8	*k_Passive*	Passive stator length	0.75	1.45

II. Motor Topology, Design Considerations, and Reference Prototype

The reference vernier machine, known as MAGNUS, which is shown in Fig. 1 has two stators, the main (active) and the auxiliary (passive) stators, each having 12 teeth and split poles. Only the main stator has a 3 phase winding and 12 coils wound on the teeth in a double-layer arrangement, and the auxiliary stator is profiled similar to the main stator, without any coils in slots. In one study on torque production of each component of the MAGNUS machine, it has been reported that the auxiliary stator produces approximately 50% as much as the torque generated by the main stator [28].

The operating principle of this machine demonstrating different slot and pole combinations have been reported in [29], and [30]. The structure of MAGNUS machine allows the use of a single coil per slot configuration, which enables the implementation of advanced cooling systems. Furthermore, the stator structure for in-wheel traction allows access to the windings on the main stator, which benefits from the ability to have direct cooling.

The rotor of the reference design has 40 PMs (poles), which are inserted into the rotor slots in a spoke configuration resulting in a high flux concentration. The model specified in this paper has been successfully designed as shown in Figs. 1a, and 1b and validated by a prototype as shown in Fig. 1c, which serves as a calibrated model for this paper.

The designs under study have three dimensional flux pathways, which necessitates a 3-D FE design, which is time consuming and requires a high computational power. Symmetric geometry and modeling the minimum periodicity region enables a more time-efficient model. In this design a quarter of the full geometry has been modelled, as shown in Fig. 2, which significantly mitigates the analysis time and effort.

III. Problem Formulation and Large-scale Differential Evolution Optimization

Various specifications for in-wheel traction motors have been considered based on the weight of the vehicle. In lightweight vehicles, those fully electric or potentially hybrid, electric motors with a peak power ranging from 20 to 40 kW are suitable. For heavier vehicles, such as passenger cars, in-wheel motors with approximately 75 kW of peak power are considered. Buses and trains may require even more torque for in-wheel motors, reaching up to 90 kW of peak power, reflecting the specific requirements of the motor technologies for in-wheel traction.

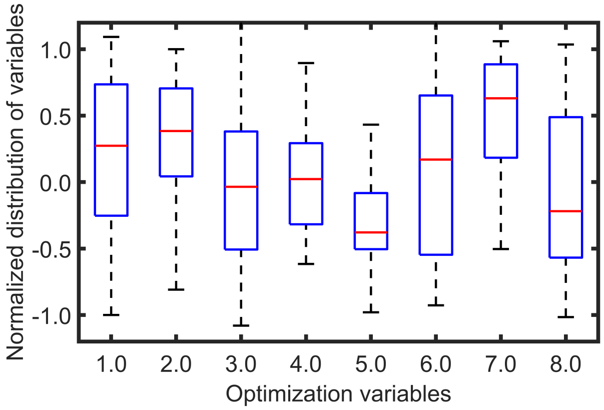

Fig. 3. Normalized distribution of independent variables of the Pareto front designs, showing that suitable ranges have been selected.

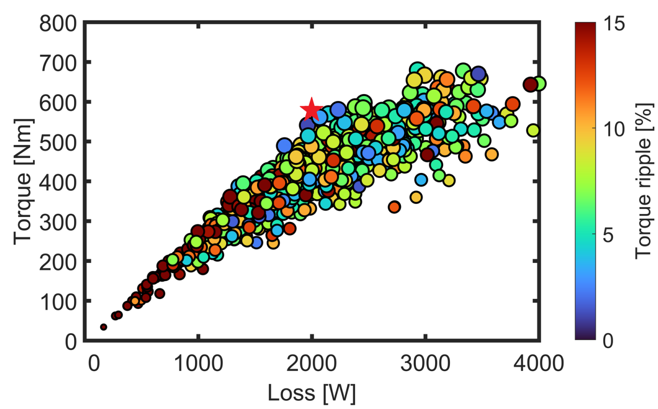

Fig. 4. Design candidates evaluated in the optimization study, with the torque ripple shown as the color map and the machine goodness as the size of the circles. The selected design is shown with a (★).

Optimization techniques are typically employed for seeking suitable designs, considering various objectives. Differential evolution (DE) is a popular population-based evolutionary optimization algorithm widely used in various fields, which involves improving a set of candidate designs over multiple cycles or generations [4], [31].

The rated power and speed for the vernier machine are considered to be 40 kW and 700 rpm, respectively. The optimization algorithm, imposed a constraint on the electromagnetic torque to be higher than 600 Nm, combined with the single objective scenario with the goal of loss minimization to improve the optimization speed.

Parameters such as the outer diameter, inner diameter, current density, and the number of magnetic poles were kept constant while other geometrical variables were systematically adjusted to target the most favorable design. The description and ranges for the independent variables, which are considered to result in geometrical robust designs are provided in Table I and shown in Fig. 2. The generated designs were evaluated through 3-D FEA simulations carried out using the Ansys Electronics Desktop 2023 software [32].

IV. Comparative Analysis and Constant Power Operation

The design selected from the optimization serves as a basis for comparative analysis. The comparison involves replacing the spoke-type rotor with a Halbach array rotor without a laminated core, and a surface-mounted PM rotor where PMs are mounted on a rotor back-iron.

In axial-flux machines the outer diameter of the electric machine has a significant effect on the electromagnetic torque, which is proportional to the outer diameter cubed. In the selected design, the outer diameter is 300 mm and to have a fair comparison between the spoke-type, Halbach array, and surface-mounted PM rotors, all the geometrical and electrical variables contributing to electromagnetic torque, for example, outer and inner diameters, coil axial length, current density, and number of turns per phase have been considered constant.

In traction application, a torque versus speed curve specifies for the torque to be constant up to the base speed, which is the speed where the machine's voltage equals the inverter's maximum voltage. To meet the voltage limitation of the inverter, constant power operation is necessary when the machine's speed surpasses the base speed.

V. Results and Discussions

The optimization results illustrating the box plot of the normalized distribution of the independent variables for the Pareto front designs are depicted in Fig. 3. The electromagnetic torque versus losses in the designed population are shown in Fig. 4, and a selected best design on the Pareto front is marked with a star. The size of each circle for the candidate designs shows its goodness, which is defined as

$$GD = \frac{T}{\sqrt{W_{Loss}}}, \quad (1)$$

where T is the electromagnetic torque and W_{Loss} is the machine losses. In designs where they have different torques it is important to have a comparison in terms of goodness [33], which takes into account the torque, losses, and therefore the efficiency of each design. The geometry of the selected design is shown in Fig. 2 and has the highest goodness among the designs on the Pareto and a suitable torque ripple below 5%.

The spoke-type and surface-mounted PM rotors use the same active and passive stators as shown in Fig. 5, whereas the Halbach array rotor only requires the active stator because the electromagnetic flux density on the other side of the rotor facing the passive stator is negligible.

The design with two back to back Halbach rotors and a passive and active stator will only increase the electromagnetic torque by about 5%. Considering the increase in material active mass and cost, the best utilization of Halbach array PM rotor for comparison is implementing a single rotor with an active stator. When comparing the results as shown in Table II, one needs to consider the fact that there are no ferromagnetic components in a Halbach rotor, and therefore this accounts as

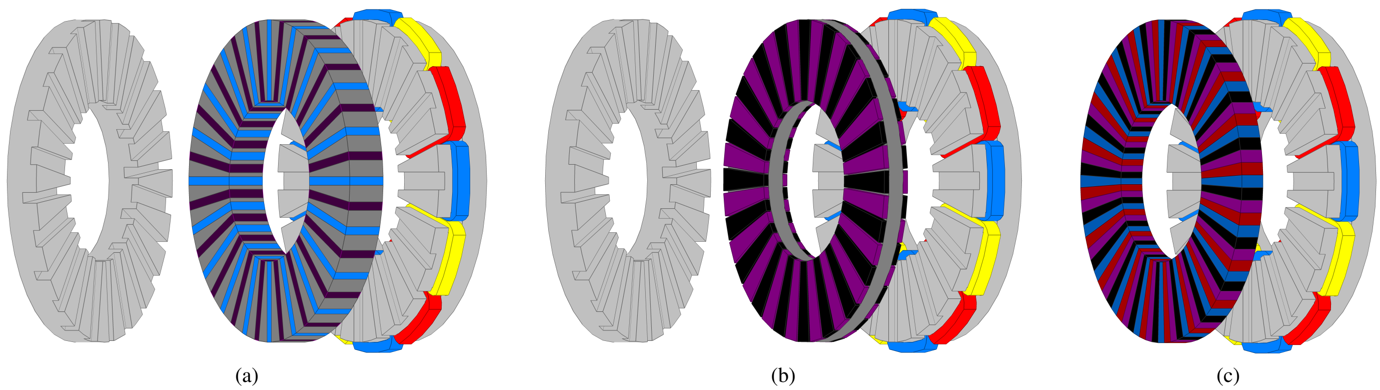

Fig. 5. The exploded view of designs with (a) spoke-type, (b) surface-mounted, and (c) Halbach array PM rotors. The active stator for all the designs is identical and located on the right hand side of the rotors. Only designs (a) and (b) have the passive stator, which is shown on the left hand side of the rotor. In design (c) only the active stator is required. A design with two back-to-back Halbach rotors with passive and active stators will only increase the electromagnetic torque by about 5%, therefore the best utilization of Halbach array PM rotor for comparison is using a single rotor with an active stator.

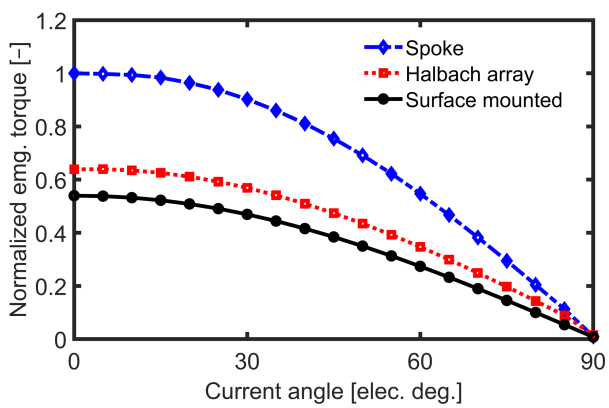

Fig. 6. The normalized electromagnetic torque versus current angle at the rated current loading shows the negligible saliency with the peak torque at $I_d = 0$. The values are normalized based on the peak torque of the vernier machine with the spoke-type rotor.

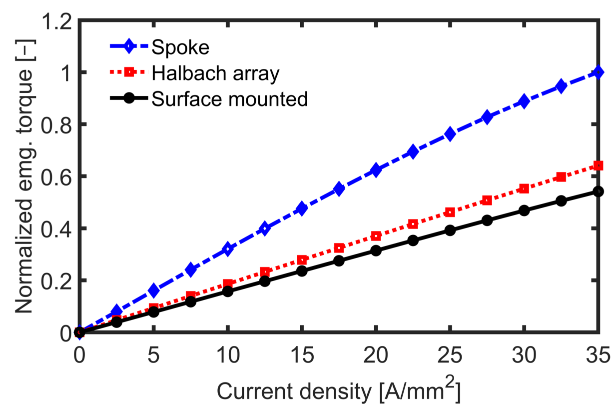

Fig. 7. The normalized electromagnetic torque versus current density shows the minimum effect of saturation in all designs. The values are normalized based on the peak torque of the vernier machine with the spoke-type rotor.

an extremely large airgap with respect to the armature reaction. The specific PM mass indicates that spoke-type rotor has the most efficient utilization of permanent magnet materials which leads to a lower active material cost.

The torque profile of the designs considered for comparison in this paper is depicted in Fig. 6, where the saliency ratio is close to one in all of them, hence, d and q-axis inductances are almost equal which can be seen in the electromagnetic torque curve where the maximum is at zero electric degrees current angle. The reported results for all the designs have been normalized based on the peak electromagnetic torque of the reference spoke-type rotor.

The normalized electromagnetic torque versus current density in Fig. 7, shows the minimal effect of saturation in the designs under study for in-wheel where the torque increases almost linearly with the current density. The torque-speed characteristics for different rotor types and the constant power region for each rotor are shown in Fig. 8. All of the designs considered for comparison in the vernier machine under study in this paper can perform flux weakening by using the current phase advance.

The flux concentration for the double stator axial-flux spoke topology can be defined as

$$\zeta_{sp} = \frac{h_{PM}}{\tau_p} = \frac{h_{PM} \cdot p}{\pi D}, \tag{2}$$

where h_{PM} is the axial length of the PM, D is the diameter, and τ_p the pole pitch, which is defined as the machine circumference πD divided by the number of poles p. The flux concentration ratio for the Halbach array PM rotor can be defined as

$$\zeta_h = \frac{2h_{PM} + \ell_{PM}}{\tau_p}, \tag{3}$$

where ℓ_{PM} is the tangential length of the PM, and for surface-mounted PM rotor the flux concentration can be calculated by

$$\zeta_s = \frac{\ell_{PM}}{\tau_p}. \tag{4}$$

To show the flux intensification capability of the designs under study, the flux concentration ratio for each design

TABLE II
PERFORMANCE OF THE DESIGNS WITH SPOKE-TYPE, HALBACH ARRAY, AND SURFACE-MOUNTED PM ROTORS. CONSIDERING THE PERFORMANCE INDICES SUCH AS EFFICIENCY, MACHINE GOODNESS, AND COST, THE DESIGN WITH SPOKE-TYPE ROTOR HAS A SUPERIOR PERFORMANCE COMPARED TO THE OTHER TYPES OF ROTORS.

Design	Peak torque [Nm]	Axial length [mm]	Efficiency [%]	Power density [kW/kg]	Specific mass [g/Nm]	Specific PM mass [g/Nm]	Goodness [kNm/$\sqrt{W_{loss}}$]	Active material cost [p.u.]
Spoke	541	120	96.7	2.11	74.56	11.91	23.41	462
Halbach	345	75	95.8	2.11	74.27	20.56	9.44	490
SPM	295	110	94.6	1.23	127.89	12.21	5.68	276

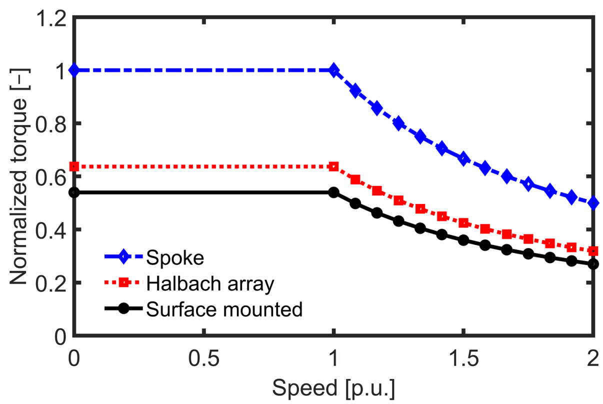

Fig. 8. Torque versus speed characteristics of the designs under study. The design with a spoke-type rotor has a higher constant power operation region, and all the designs can maintain constant power.

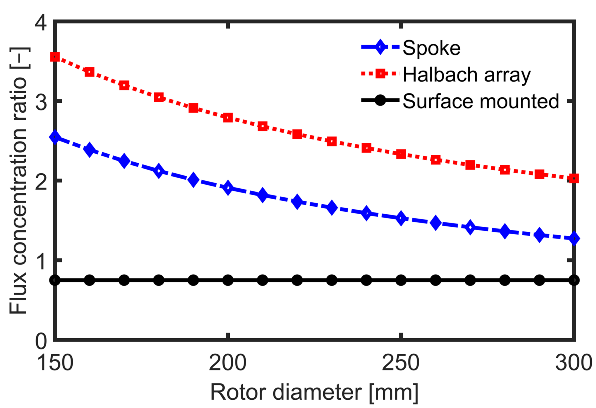

Fig. 9. Flux concentration ratio of the studied designs versus rotor diameter. The Halbach array rotor with an axially magnetized PM placed between two spoke PMs shows a high flux concentration.

is as shown in Fig. 9. The results indicate the Halbach array rotor has a high flux concentration and therefore a comparable power density to design with spoke rotor. The special configuration of a Halbach rotor where an axially magnetized PM in placed between two spoke PMs enables such a high flux intensification capability. Performance of the design considered for comparison has been reported in Table II, where the results indicate the significant advantage of implementing spoke-type rotor in vernier machines with active and passive stators.

VI. CONCLUSION

The axial-flux PM vernier machine known as MAGNUS was successfully optimized for in-wheel traction. Using the minimum region of periodicity in FE design and single objective problem combined with a constraint increased the speed of optimization algorithm. A best design of the Pareto front was selected to compare three rotor designs, namely, spoke, Halbach array, and surface-mounted PM. Multiple parametric studies were conducted and it was shown that spoke-type rotor has a superior performance and can maintain a higher constant power operation region.

The flux concentration ratio calculation methods for each rotor type were introduced and parametric study results indicated a significant flux concentration capability for the Halbach array PM rotor. A summary of the performance of each design considering multiple indices such as efficiency, goodness, power density and cost showed the superiority of the design with the spoke-type PM rotor.

ACKNOWLEDGMENT

This paper is based upon work supported by the National Science Foundation (NSF) under Award No. #1809876. Any opinions, findings, conclusions, or recommendations expressed in this material are those of the authors and do not necessarily reflect the views of the NSF. The support of Ansys Inc., and of University of Kentucky, the L. Stanley Pigman Chair in Power Endowment is also gratefully acknowledged.

REFERENCES

[1] B. Fahimi, L. H. Lewis, J. M. Miller, S. D. Pekarek, I. Boldea, B. Ozpineci, K. Hameyer, S. Schulz, A. Ghaderi, M. Popescu, B. Lehman, and D. D. Patel, "Automotive Electric Propulsion Systems: A Technology Outlook," *IEEE Transactions on Transportation Electrification*, pp. 1–1, 2023.

[2] T. Woolmer and M. McCulloch, "Analysis of the yokeless and segmented armature machine," in *2007 IEEE International Electric Machines & Drives Conference*, vol. 1, 2007, pp. 704–708.

[3] A. Allca-Pekarovic, P. J. Kollmeyer, A. Forsyth, and A. Emadi, "Experimental Characterization and Modeling of a YASA P400 Axial Flux PM Traction Machine for Performance Analysis of a Chevy Bolt EV," *IEEE Transactions on Industry Applications*, pp. 1–11, 2023.

[4] M. Rosu, P. Zhou, D. Lin, D. M. Ionel, M. Popescu, F. Blaabjerg, V. Rallabandi, and D. Staton, *Multiphysics Simulation by Design for Electrical Machines, Power Electronics and Drives*. J. Wiley - IEEE Press, 2017.

[5] A. Mohammadi, Y. Chulaee, A. M. Cramer, I. G. Boldea, and D. M. Ionel, "Axial Flux Permanent Magnet Vernier Machine with Single-wound Dual-stator and Spoke Permanent Magnet Rotor for Electric Vehicle In-wheel Traction," in *2023 IEEE Transportation Electrification Conference & Expo (ITEC)*, 2023, pp. 1–5.

[6] C. S. Goli, M. Salehi, S. Essakiappan, D. M. Ionel, J. Gafford, and M. Manjrekar, "Comparative Analysis of Doubly Salient Special Machine and Flux Switching Machine with PMs in Stator," in *2023 IEEE International Electric Machines & Drives Conference (IEMDC)*, 2023, pp. 1–7.

[7] K. Chen and B. Sarlioglu, "Vernier Machine Analysis and Analytical Design for Traction Applications," in *2021 International Aegean Conference on Electrical Machines and Power Electronics (ACEMP) & 2021 International Conference on Optimization of Electrical and Electronic Equipment (OPTIM)*, 2021, pp. 426–431.

[8] Y. Gao, T. Kosaka, and R. Qu, "Comparative Study of High-Current-Density High-Speed Vernier Permanent Magnet Machines for Electric Vehicle Traction Application," in *2022 International Conference on Electrical Machines (ICEM)*, 2022, pp. 1899–1905.

[9] S. Cai, J. L. Kirtley, and C. H. T. Lee, "Critical Review of Direct-Drive Electrical Machine Systems for Electric and Hybrid Electric Vehicles," *IEEE Transactions on Energy Conversion*, vol. 37, no. 4, pp. 2657–2668, 2022.

[10] Y. Zhao, D. Li, Z. Liang, and R. Qu, "A high power factor pm vernier machine with segmented-stator," *IEEE Transactions on Transportation Electrification*, pp. 1–1, 2024.

[11] A. Allahyari, E. Bostanci, and A. Mahmoudi, "High-Performance Vernier Machines with Halbach Array Permanent Magnets for Direct Drive Applications," *Machines*, vol. 11, no. 5, 2023. [Online]. Available: https://www.mdpi.com/2075-1702/11/5/525

[12] Y. Yu, X. Zhang, F. Chai, Y. Pei, L. Chen, and M. Doppelbauer, "Tradeoff Study of Torque and Losses in Permanent Magnet Vernier and Synchronous Machines for In-Wheel Traction Applications," *IEEE Transactions on Industry Applications*, vol. 60, no. 1, pp. 400–410, 2024.

[13] D. M. Ionel, J. F. Eastham, and T. Betzer, "Finite element analysis of a novel brushless DC motor with flux barriers," *IEEE Transactions on Magnetics*, vol. 31, no. 6, pp. 3749–3751, 1995.

[14] D. M. Ionel, D. C. Jackson, G. Starr, and A. P. Turner, "Permanent magnet brushless motors for industrial variable speed drives," in *2002 International Conference on Power Electronics, Machines and Drives (Conf. Publ. No. 487)*, 2002, pp. 650–654.

[15] A. Mohammadi, O. A. Badewa, Y. Chulaee, D. M. Ionel, S. Essakiappan, and M. Manjrekar, "Direct-Drive Wind Generator Concept with Non-Rare-Earth PM Flux Intensifying Stator and Reluctance Outer Rotor," in *2022 11th International Conference on Renewable Energy Research and Application (ICRERA)*, 2022, pp. 582–587.

[16] S. Sheshaprasad, M. Johnson, and H. A. Toliyat, "Design Optimization of Radial Flux-Focusing Coaxial Magnetic Gears and Comparison with Conventional Surface Permanent Magnet and Halbach Topologies," in *2023 IEEE Energy Conversion Congress and Exposition (ECCE)*, 2023, pp. 4580–4587.

[17] S. Yousefnejad, H. Heydari, K. Akatsu, and J.-S. Ro, "Analysis and Design of Novel Structured High Torque Density Magnetic-Geared Permanent Magnet Machine," *IEEE Access*, vol. 9, pp. 64 574–64 586, 2021.

[18] W. Guendouz, A. Tounzi, and T. Rekioua, "Design of Quasi-Halbach Permanent-Magnet Vernier Machine for Direct-Drive Urban Vehicle Application," *Machines*, vol. 11, no. 2, 2023. [Online]. Available: https://www.mdpi.com/2075-1702/11/2/136

[19] M. Vatani, A. Mohammadi, D. Lewis, J. F. Eastham, and D. M. Ionel, "Coreless Axial Flux Halbach Array Permanent Magnet Generator Concept for Direct-Drive Wind Turbine," in *2023 12th International Conference on Renewable Energy Research and Applications (ICRERA)*, 2023, pp. 612–617.

[20] Y. Zhao, D. Li, X. Ren, Z. Liang, and R. Qu, "Low Pole-Pair Ratio Integration Design of Permanent Magnet Vernier Machine With Improved Power Factor," *IEEE Transactions on Industrial Electronics*, vol. 71, no. 3, pp. 2820–2830, 2024.

[21] P. M. Tlali, R. Wang, and S. Gerber, "Comparison of PM Vernier and Conventional Synchronous 15 kW Wind Generators," in *Proc. Int. Conf. Electr. Mach. (ICEM)*, Sep. 2018, pp. 2065–2071.

[22] V. Rallabandi, N. Taran, D. M. Ionel, and I. G. Boldea, "MAGNUS — an ultra-high specific torque PM axial flux type motor with flux focusing and modulation," in *2017 IEEE Energy Conversion Congress and Exposition (ECCE)*, 2017, pp. 1234–1239.

[23] R. Zhang, J. Li, R. Qu, and D. Li, "Analysis and Design of Triple-Rotor Axial-Flux Spoke-Array Vernier Permanent Magnet Machines," *IEEE Transactions on Industry Applications*, vol. 54, no. 1, pp. 244–253, 2018.

[24] D. Li, R. Qu, and T. A. Lipo, "High-Power-Factor Vernier Permanent-Magnet Machines," *IEEE Transactions on Industry Applications*, vol. 50, no. 6, pp. 3664–3674, 2014.

[25] D. Li, R. Qu, W. Xu, J. Li, and T. A. Lipo, "Design Procedure of Dual-Stator Spoke-Array Vernier Permanent-Magnet Machines," *IEEE Transactions on Industry Applications*, vol. 51, no. 4, pp. 2972–2983, 2015.

[26] L. Xu, G. Liu, W. Zhao, J. Ji, and X. Fan, "High-Performance Fault Tolerant Halbach Permanent Magnet Vernier Machines for Safety-Critical Applications," *IEEE Transactions on Magnetics*, vol. 52, no. 7, pp. 1–4, 2016.

[27] D. K. Jang and J. H. Chang, "Design of a Vernier Machine with PM on Both Sides of Rotor and Stator," *IEEE Transactions on Magnetics*, vol. 50, no. 2, pp. 877–880, 2014.

[28] M. G. Kesgin, P. Han, D. Lawhorn, and D. M. Ionel, "Analysis of torque production in axial-flux vernier pm machines of the magnus type," in *2021 IEEE International Electric Machines & Drives Conference (IEMDC)*, 2021, pp. 1–5.

[29] V. Rallabandi, N. Taran, D. M. Ionel, and I. G. Boldea, "Axial-flux PM synchronous machines with air-gap profiling and very high ratio of spoke rotor poles to stator concentrated coils," in *2017 IEEE International Electric Machines and Drives Conference (IEMDC)*. IEEE, 2017, pp. 1–7.

[30] A. Mohammadi, Y. Chulaee, A. M. Cramer, I. G. Boldea, and D. M. Ionel, "Parameter Identification, Non-linearity, and Harmonic Effects in a Vernier Machine of the MAGNUS Type," in *2023 IEEE Energy Conversion Congress and Exposition (ECCE)*, 2023, pp. 4286–4291.

[31] R. Storn and K. Price, "Differential Evolution – A Simple and Efficient Heuristic for global Optimization over Continuous Spaces," in *Journal of Global Optimization*, vol. 11, 1997, pp. 341–359.

[32] *Ansys® Electronics, Maxwell, version 23.2, 2023, ANSYS Inc.*

[33] Y. Wang, D. M. Ionel, V. Rallabandi, M. Jiang, and S. J. Stretz, "Large-Scale Optimization of Synchronous Reluctance Machines Using CE-FEA and Differential Evolution," *IEEE Transactions on Industry Applications*, vol. 52, no. 6, pp. 4699–4709, 2016.